AD-A266 851

# XPS Analysis of Al/EPDM Bondlines from IUS SRM-1 Polar Bosses: Final Report

Prepared by

C. S. HEMMINGER and N. MARQUEZ
Mechanics and Materials Technology Center
Technology Operations

10 March 1993

Prepared for

SPACE AND MISSILE SYSTEMS CENTER
AIR FORCE MATERIEL COMMAND
Los Angeles Air Force Base
P. O. Box 92960
Los Angeles, CA 90009-2960

Programs Group

THE AEROSPACE CORPORATION
El Segundo, California

93-15860

Lt. Col. N. Compton
SMC/CLU

Wm. Kyle Sneddon, Capt., USAF
Deputy Chief
Industrial & International Programs Division

## REPORT DOCUMENTATION PAGE

| 1a. REPORT SECURITY CLASSIFICATION<br>Unclassified | 1b. RESTRICTIVE MARKINGS |
|---|---|
| 2a. SECURITY CLASSIFICATION AUTHORITY | 3. DISTRIBUTION/AVAILABILITY OF REPORT |
| 2b. DECLASSIFICATION/DOWNGRADING SCHEDULE | Approved for public release; distribution unlimited |

| 4. PERFORMING ORGANIZATION REPORT NUMBER(S)<br>TR-93(3464)-1 | 5. MONITORING ORGANIZATION REPORT NUMBER(S)<br>SMC-TR-93-28 |
|---|---|

| 6a. NAME OF PERFORMING ORGANIZATION<br>The Aerospace Corporation<br>Technology Operations | 6b. OFFICE SYMBOL<br>(If applicable) | 7a. NAME OF MONITORING ORGANIZATION<br>Space and Missile Systems Center |
|---|---|---|
| 6c. ADDRESS (City, State, and ZIP Code)<br>El Segundo, CA 90245-4691 | | 7b. ADDRESS (City, State, and ZIP Code)<br>Los Angeles Air Force Base<br>Los Angeles, CA 90009-2960 |

| 8a. NAME OF FUNDING/SPONSORING ORGANIZATION | 8b. OFFICE SYMBOL<br>(If applicable) | 9. PROCUREMENT INSTRUMENT IDENTIFICATION NUMBER<br>F04701-88-C-0089 |
|---|---|---|

| 8c. ADDRESS (City, State, and ZIP Code) | 10. SOURCE OF FUNDING NUMBERS | | | |
|---|---|---|---|---|
| | PROGRAM ELEMENT NO. | PROJECT NO. | TASK NO. | WORK UNIT ACCESSION NO. |
| | | | | |

**11. TITLE (Include Security Classification)**

XPS Analysis of Al/EPDM Bondlines from IUS SRM-1 Polar Bosses: Final Report

**12. PERSONAL AUTHOR(S)**
Hemminger, Carol S. and Marquez, Nicholas

| 13a. TYPE OF REPORT | 13b. TIME COVERED<br>FROM _____ TO _____ | 14. DATE OF REPORT (Year, Month, Day)<br>1993 March 10 | 15. PAGE COUNT<br>20 |
|---|---|---|---|

**16. SUPPLEMENTARY NOTATION**

| 17. COSATI CODES | | | 18. SUBJECT TERMS (Continue on reverse if necessary and identify by block number) |
|---|---|---|---|
| FIELD | GROUP | SUB-GROUP | Polar Boss<br>Metal /Rubber Bonding<br>Corrosion |
| | | | |

**19. ABSTRACT (Continue on reverse if necessary and identify by block number)**

A temperature-stress rupture method using partial immersion in liquid nitrogen has been developed for the aluminum/EPDM rubber insulation bondline of the IUS SRM-1 polar bosses in order to investigate a corrosion problem. Subsequent XPS analysis of the ruptured bondline followed changes in the locus of failure as corrosion progressed. Samples from the forward polar bosses had a predominantly noncorroded appearance on the ruptured surfaces. The locus of failure was predominantly through the primer layer, which is distinguished by a high concentration of chlorinated hydrocarbon. The aft polar boss segments analyzed were characterized by the presence of corrosion over the entire mid-section of the ruptured aluminum to insulation bondline. The predominant corrosion product detected was aluminum oxide/hydroxide. The corroded bondline sections had significantly higher concentrations of aluminum oxide/hydroxide than the noncorroded areas, and lower concentrations of primer material. The temperature-stress rupture appeared to progress most readily through areas of thickened aluminum oxide/hydroxide infiltrated into the primer layer. In general there was a very good correlation between the calculated Cl:Al atomic % ratio, and the visual

| 20. DISTRIBUTION/AVAILABILITY OF ABSTRACT<br>[X] UNCLASSIFIED/UNLIMITED ☐ SAME AS RPT. ☐ DTIC USERS | 21. ABSTRACT SECURITY CLASSIFICATION<br>Unclassified |
|---|---|
| 22a. NAME OF RESPONSIBLE INDIVIDUAL | 22b. TELEPHONE (Include Area Code)     22c. OFFICE SYMBOL |

DD FORM 1473, 84 MAR     83 APR edition may be used until exhausted.<br>All other editions are obsolete.     SECURITY CLASSIFICATION OF THIS PAGE

UNCLASSIFIED

characterization of the extent of corrosion. The Cl:Al ratio, which represents the primer to corrosion product ratio at the locus of failure, varied from 0.4 to 47. With only a few exceptions, surfaces with a predominantly noncorroded appearance had Cl:Al ratios > 2, and surfaces with a heavily corroded appearance had Cl:Al ratios < 1. The ID edges and wingtip edges of the aft segments appeared generally less corroded than the mid-sections, but the XPS data suggested that the surface composition analysis technique is a more sensitive probe of the extent of corrosion at the bondline than a visual inspection of the ruptured surfaces. XPS did not detect chloride ion mixed with the chlorine-bonded-to-carbon from the primer on any of the polar boss samples, but its presence at low concentration was not ruled out.

# PREFACE

|  | | |
| --- | --- | --- |
| **Accession For** | | |
| NTIS GRA&I | ☑ | |
| DTIC TAB | ☐ | |
| Unannounced | ☐ | |
| Justification | | |
| By | | |
| Distribution/ | | |
| Availability Codes | | |
| Dist | Avail and/or Special | |
| A-1 | | |

1

# CONTENTS

# FIGURES

# TABLES

## BACKGROUND

The IUS Program is investigating recertification of two SRM-1 motors beyond the ten-year specification limit warranted by Chemical Systems Division (CSD). The two motors will be over ten years old on scheduled launch dates, and replacement motors are not readily available. It was determined by Boeing and CSD during destructive testing that the motors were not age-sensitive except for a corrosion problem at the insulation-to-aluminum polar boss bondlines. Failure at this bondline during firing would result in catastrophic loss. The first investigative team suggested that improper environmental storage conditions for the test motors were the sole cause of bondline corrosion and that flight motors were not at risk.

Corrosion and minor insulator debonds were observed on the aluminum polar bosses of three old motor cases. Rejected flight motor cases S/Ns 114 and 029 were selected for skirt proof load and hydroburst tests. S/N 126 was used as pathfinder to cut peel test samples for test articles. Corrosion and debonds were discovered on S/N 114 prior to test, but it was used "as-is," since no effect was anticipated on the test objectives. The critical polar boss ID bondline did not appear to be compromised, with peel strengths meeting operational requirements. Corrosion and hidden debonds were detected later on S/N 029 upon destructive and nondestructive physical analysis, but corrosion was judged minor compared to S/N 114. Both S/N 114 and 029 successfully completed the skirt proof load and hydroburst tests. Only minor corrosion has been found on S/N 126. The peel strengths on S/Ns 029 and 126 were unaffected, and had a high margin of acceptance.

Unlike flight hardware that is stored under controlled conditions, the S/N 114 and 029 motor cases subjected to destructive analysis had been stored in uncontrolled environments with high humidity exposures. For example, rejected flight motor case S/N 114 spent 14.5 months in Seattle, Washington, in a crate stored outdoors through two winters. CSD anecdotal information on S/Ns 029 and 126 indicated significantly less severe storage environments. It was thought that the atypical moisture exposures caused initiation and progression of the corrosion and debonds observed at the aluminum polar boss-to-insulation bondlines.

A method for the analysis of steel-to-rubber bondlines[1] was developed in the Materials Sciences Laboratory of The Aerospace Corporation in 1989. This method used rapid immersion of samples in liquid nitrogen to rupture the metal-to-rubber bondline predominantly near the metal/primer interface. The temperature stress takes advantage of the differences in the coefficients of thermal expansion of the materials at the bondline. The primer is relatively brittle compared to the adhesive and rubber layers, so it was not surprising that the rupture was observed at this layer. The liquid nitrogen blanketed the ruptured surfaces from air exposure, and made it possible to transfer the samples to an inert atmosphere dry box with minimal surface oxidation from moisture or oxygen. Subsequent analysis of both sides of the ruptured steel-to-rubber bondlines were made by x-ray photoelectron spectroscopy (XPS). XPS surface composition and chemistry results for ruptured steel/rubber bondlines determined the locus of failure, and gave insight into the steel-to-primer adhesion and aging properties.

A temperature-stress-rupture method followed by XPS analysis would be equally useful in the study of the IUS polar boss samples. In the SRM-1 production, ethylene propylene diene monomer (EPDM) rubber is bonded to aluminum alloy 7175-T736 with Chemlok 205 primer and Chemlok 234B adhesive. Until this study, no method had been reported for the rupture or analysis of Al/EPDM rubber bondlines beyond standard peel, pull, or blister tests. Cohesive failure in the rubber occurs during such tests if a good adhesive bond has been fabricated. Even poor bonds, such as those discovered on the aft polar boss of S/N 114, gave large areas of cohesive failure during a peel

5

test. The areas of cohesive failure complicated analysis and data interpretation. It was therefore proposed that samples from the IUS SRM-1 polar bosses of motor cases S/Ns 114, 029, and 126 be made available to The Aerospace Corporation for the development of a temperature-stress-rupture method, and subsequent surface analysis. It was considered particularly desirable to analyze both corroded and noncorroded bondlines. The initial results, for about half of the samples, were reported in February, 1992.[2] A proposal was also made to use this method to directly study the effect of water on EPDM rubber/Al bonded with the Chemlok adhesive system.[3] The final report[4] was completed for this test program in September, 1992.

## EXPERIMENTAL

Ten segments from five polar bosses were made available from the motor case hardware, as shown in Table I. There were two segments cut from each forward and aft polar boss of motor cases S/Ns 114 and 029, a third segment from the S/N 114 aft polar boss (including peel-tested areas of a corroded zone), and one segment cut from the aft polar boss of S/N 126. The segment dimensions vary because the polar bosses differ in size, as indicated in Table I by the boss diameter measured across the bolt circle. The lengths of the cut segments are indicated approximately in circumferential inches.

Samples were cut from each polar boss segment to prepare coupons of size and shape appropriate for rupture and analysis. The first step was to saw-cut a slice, of approximately 0.5 circumferential inches, off one end of each segment . A polar boss slice is shown schematically in Fig. 1. Slices from the forward and aft bosses of S/N 114 are shown in Fig. 2; slices from the forward and aft bosses of S/N 029 are shown in Fig. 3. The forward bosses are threaded to accept the igniter assembly. The insulation and Al of each slice were trimmed to about 0.125 inch thick, to give a "sandwich" about 0.25 inch thick. The "sandwich" was then cut lengthwise into four coupons, which ranged from about 0.5 x 0.5 x 0.25 inch to 0.5 x 1.0 x 0.25 inch in size, depending on the diameter of the polar boss. This is shown schematically in Fig. 1. The two edges of the polar boss radial strip are referred to as the ID edge, exposed directly to the environment, and the wingtip, buried between the EPDM rubber and sheer ply insulation layers.

Table I. Segments of Polar Boss Available for Analysis

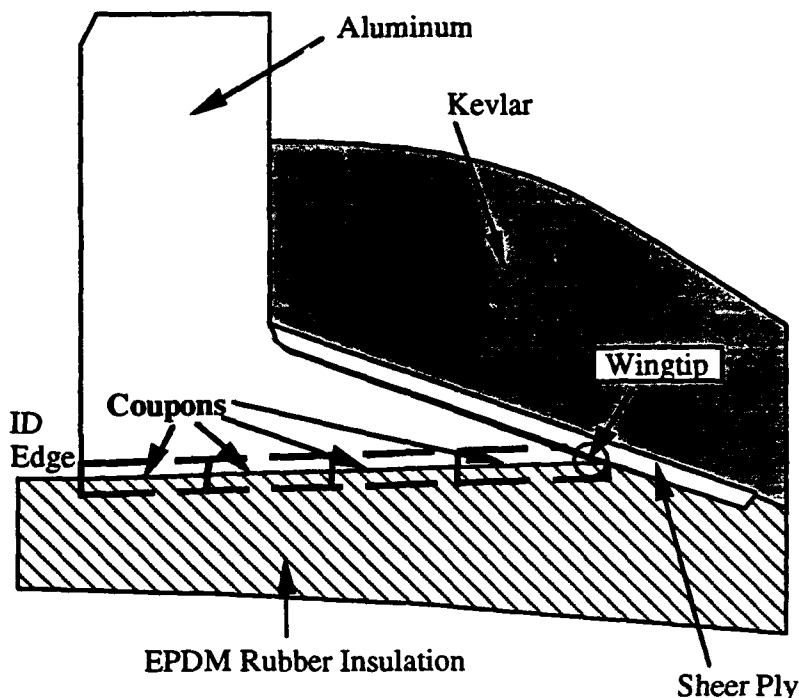| Spec. No. | S/N | Polar Boss | Boss Diameter (in.) | Location on Polar Boss (Top Dead Center at 0°) | Length (in.) |
|---|---|---|---|---|---|
| A5 | 114 | Forward | 14.6 | Unknown | ~2 |
| A6 | 114 | Forward | | Unknown: ~ 90° from A5 | ~2 |
| A1 | 114 | Aft | 28.8 | ~330° | ~2 |
| A2 | 114 | Aft | | ~210° | ~2 |
| A12 | 114 | Aft | | Unknown: includes peel strips 1-6 | ~7 |
| A7 | 029 | Forward | 11.4 | ~180° | ~2 |
| A8 | 029 | Forward | | Top Dead Center | ~2 |
| A3 | 029 | Aft | 19.1 | ~330° | ~2 |
| A4 | 029 | Aft | | ~30° | ~2 |
| A9 | 126 | Aft | 28.8 | ~270° | ~5 |

Figure 1. Schematic of polar boss slice, showing coupons for temperature-stress rupture.

Rapid immersion of an entire coupon into liquid nitrogen did not result in rupture. Rupture could be made predominantly near the Al/Chemlok 205 Primer interface by rapid immersion in liquid helium or by holding the Al side of the sandwich in contact with liquid nitrogen. The latter technique required careful application and did not always rupture the entire bondline, but was considerably easier to apply to a large number of samples than liquid helium immersion. Rupture was often heard as a faint crackling noise. It was also noted that a localized boiling of the liquid nitrogen was observed around the aluminum just before rupture; this was a more reliable indicator than the sound of rupture. It was typically necessary to use fine-tip tweezers at the edge of the bondline to separate the two halves after rupture. This was easiest after warming the sample to room temperature, but could usually be accomplished in the liquid nitrogen, if desired. If rupture was not complete, the two halves were pulled apart, resulting in cohesive failure in the rubber in nonruptured areas. The nonruptured area was < 10% of the total area in most samples, and did not interfere with subsequent analysis.

In cases where minimum exposure of the ruptured bondline to moisture and oxygen was desired, the entire sample was dropped into the liquid nitrogen as soon as rupture had occurred. Excess liquid nitrogen was decanted into a second dewar and the dewar with immersed sample was then introduced into the antechamber of a dry box where the remaining liquid nitrogen could be pumped away by the rough pump (this sometimes took several hours, even for small volumes; pump-down time was minimized by tilting the dewar onto one side to increase the liquid nitrogen surface area). The samples could subsequently be mounted for analysis and transferred to the XPS instrument under dry argon.
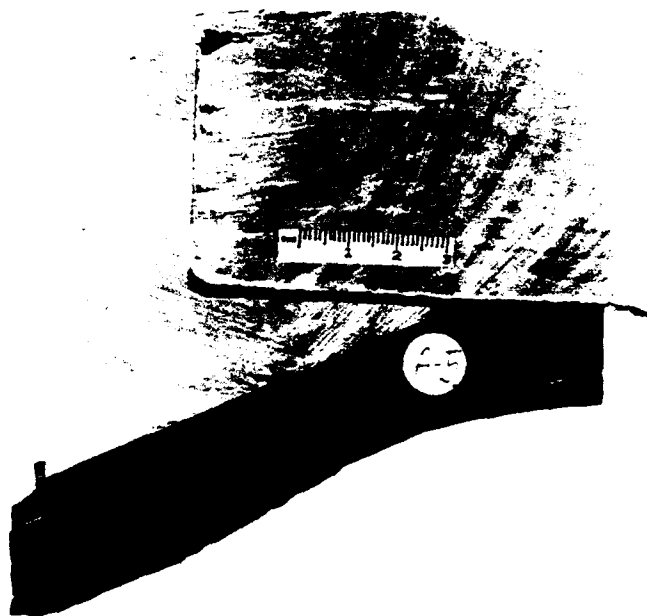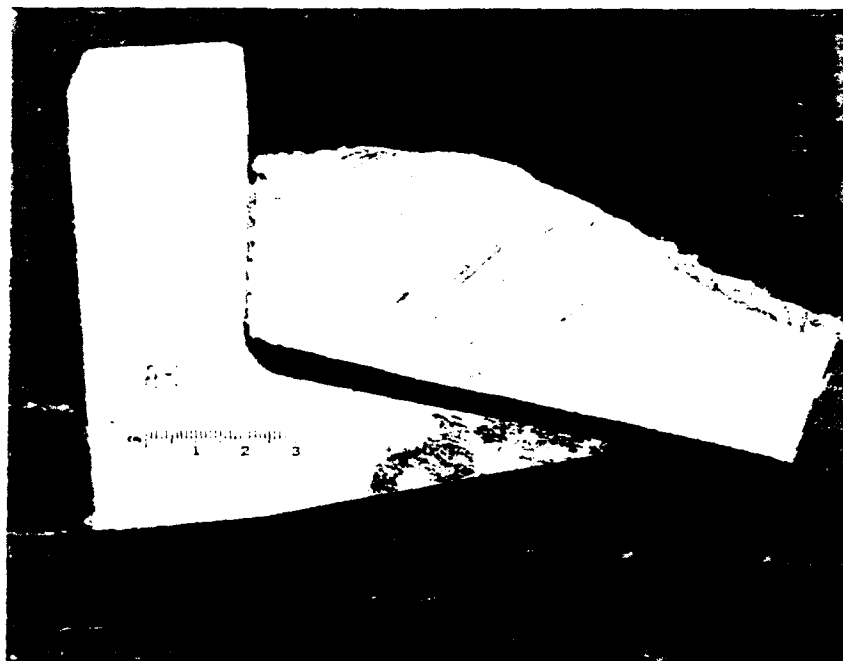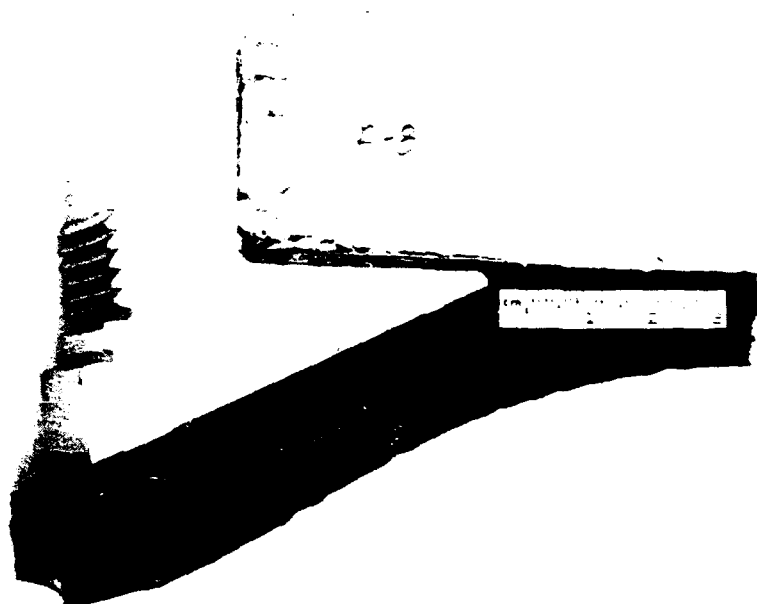
Figure 2.  Polar boss slices from motor case S/N 114.  a)  Forward boss.  b) Aft boss.
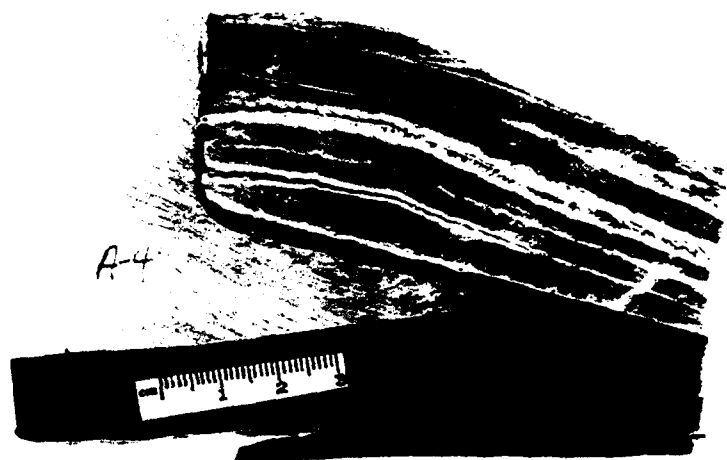
a



b



Figure 3. Polar boss slices from motor case S/N 029.  a)  Forward boss.  b) Aft boss.

Reference samples of all known starting materials were also prepared for analysis. These included the aluminum alloy, EPDM rubber, Chemlok 205 primer, and Chemlok 234B adhesive. A fresh saw-cut surface from one of the polar bosses was used as a sample of aluminum alloy 7175-T736. It was ultrasonically cleaned in 1,1,1-trichloroethane, then acetone, rinsed with acetone, and dried before analysis. A freshly cut insulation surface (made using an acetone-cleaned Exacto blade) from one of the polar boss samples was used as a reference material for EPDM rubber. Chemlok 205 primer and Chemlok 234B adhesive surfaces were prepared from fresh lots of material supplied by Lord Corporation (manufactured November, 1991; guaranteed shelf life of one year). The primer was agitated in the can, then stirred thoroughly before brushing onto stainless steel shim coupons. It was dark grey in color. Curing was done in a vacuum oven for 65 min at 201°F, followed by 120 min at 309°F. This procedure was consistent with the specifications governing the bonding between the EPDM rubber insulation and the aluminum polar bosses in the IUS flight hardware.[5] The Chemlok 234B adhesive surface was prepared and cured simultaneously, using the above technique. The adhesive was black in color. One sample surface each of primer and adhesive was gently scraped with an acetone-cleaned Exacto knife blade to provide roughened surfaces for comparison with the as-cured surfaces. Some flaking of the Chemlok 205 and 234B was observed upon scraping.

The polar boss and reference samples were analyzed by XPS using a VG Scientific LTD ESCALAB MK II instrument . The samples were mounted on sample stubs with double-sided tape. Survey scans from 0 to 1100 eV binding energy were acquired to qualitatively determine the sample surface composition. Analysis areas were about 4 x 5 mm in size and analysis depth was about 50 - 100 Å. Data acquisition with a Mg Kα source was used to check for all the elements of interest. High resolution elemental scans were subsequently run to obtain semi-quantitative elemental analyses from peak area measurements and chemical state information from the details of binding energy and shape. Measured peak areas for all detected elements were corrected by elemental sensitivity factors before normalization to give surface atom %. The quantitation error on a relative basis is ≤10% of the measurement for components with a surface concentration >1 atom %. Large uncertainties in the relative elemental sensitivity factors can introduce absolute errors of a factor of two or even greater. The detection limit is about 0.1 surface atom %, but spectral overlaps between large peaks and small peaks can make it impossible to detect minor components, particularly when more than one chemical state is present for a given element.

## RESULTS AND DISCUSSION

### Reference Materials

The XPS surface composition data for the reference samples are shown in Table II. The nominal composition of 7175 aluminum alloy by weight is 90% Al, 5.6% Zn, 2.5% Mg, 1.6% Cu, and 0.23% Cr. The fresh saw-cut surface analyzed by XPS has an aluminum oxide surface layer < 100 Å thick: both zerovalent aluminum and aluminum oxide contributions were detected for the Al2p high resolution elemental peak. The carbonaceous contamination is thin (< 20 Å). A significant surface concentration of nitrogen (1%) is detected. The Mg, Cu, and Cr components of the alloy were not detected by XPS on this surface. A freshly grit-blasted aluminum alloy surface was not analyzed for comparison, but it would be expected to have similar surface composition.

The EPDM rubber insulation is primarily hydrocarbon in content, as reflected by the surface carbon concentration of 95 atom %. It has a silica hydrate filler, and low chlorine and sulfur concentrations. Both the primer and adhesive are characterized by relatively high concentrations of

10

Table II. XPS Results: Composition of Reference Materials

| Sample Description | Surface Atom Percent, Normalized | | | | | | | | |
|---|---|---|---|---|---|---|---|---|---|
| | Al | O | Si | Zn | Cl | S | C | N | Ti |
| 7175-T736 Aluminum Alloy | 28 | 45 | nd | 0.1 | 0.3 | 0.2 | 24 | 1.0 | nd |
| EPDM Insulation | nd | 2.8 | 1.6 | tr | 0.3 | 0.2 | 95 | 0.1 | nd |
| Chemlok: | | | | | | | | | |
| 205 Primer, As Cured | nd | 11 | 3.2 | 0.2 | 17 | tr | 68 | 0.8 | nd |
| 205 Primer, Scraped Surface | 0.4 | 11 | 0.9 | 0.3 | 18 | tr | 68 | 0.6 | 0.2 |
| 234B Adhesive, As Cured | nd | 2.9 | 0.9 | nd | 11 | nd | 85 | 0.2 | nd |
| 234B Adhesive, Scraped Surface | 0.2 | 8.4 | 1.9 | nd | 9.6 | 0.2 | 78 | 0.3 | nd |

Note: tr = trace and nd = not detected

chlorinated hydrocarbon. XPS did not detect chloride ion mixed with the chlorine-bonded-to-carbon, but its presence below the detection limit is possible. The primer contains zinc and titanium oxides (the latter detected by XPS only on the scraped surface) among its suspended solids while the adhesive does not. The nitrogen concentration was higher in the primer than in the adhesive. The as-cured surfaces and the scraped surfaces (representing "bulk" material) of the primer and adhesive were similar. Significant differences were observed in the concentration of the suspended solids, and in the presence of contaminants on the scraped surfaces (including exposed steel shim substrate material).

## Polar Boss Samples

Visual inspection of the ruptured polar boss sample bondlines showed that rupture appeared to occur predominantly close to the Al/primer interface. Significant flecks of primer/adhesive did remain on the Al surface. On ruptured "good" bonds there was no visual sign of Al surface corrosion, even after the ruptured bondline was exposed to atmosphere for several weeks; the EPDM side of the rupture appeared uniformly dark grey in color. A good bondline is shown in Fig. 4, from the S/N 029 forward polar boss midsection (segment A8). Ruptured "poor" bonds had a spotted appearance on both the Al and EPDM sides of the interface, and a high density of corrosion product was observed on both surfaces under an optical microscope. Poor bondlines are shown in Fig. 5. The S/N 114 aft polar boss bondlines were mottled in appearance (Fig 5a, from segment A2), and the areas of corrosion product were large and dense (most readily seen on the rubber side). An area of cohesive failure in the rubber is seen at the wingtip edge, to the left, in Fig. 5a. The S/N 029 aft polar boss bondlines had a more uniform darkening of the Al surface (Fig 5b, from segment A3), and the areas of corrosion product were numerous and relatively small. Some ruptured bondlines were considered "fair" in appearance. The fair bondlines had a lightly mottled Al surface, but the rubber surface appeared relatively clean; small patches of corrosion product were observed on both surfaces under an optical microscope. A fair bondline is shown in Fig. 6a, from the S/N 126 aft polar boss midsection

11

EPDM Rubber Side                    Aluminum Side
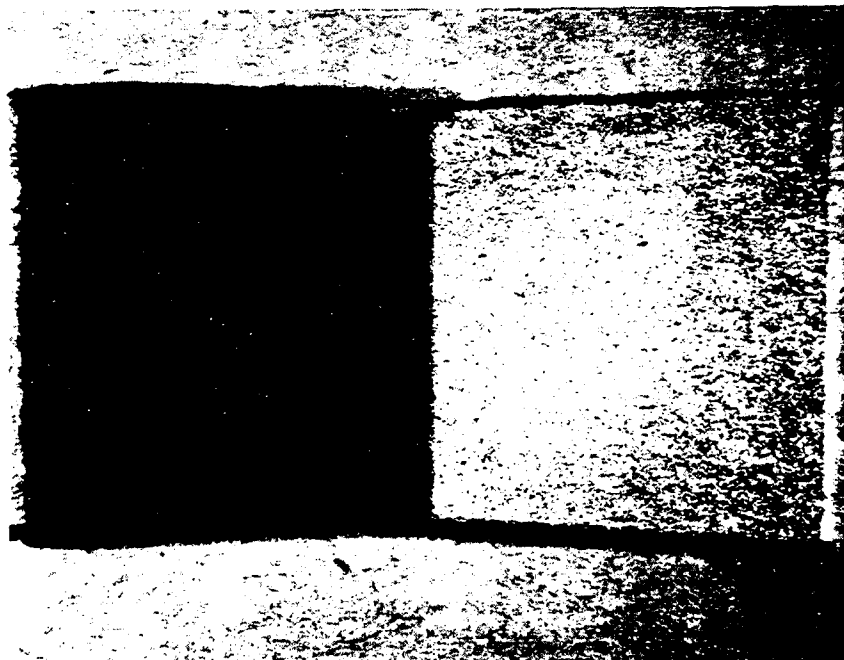


zure 4. Ruptured "good" bondline from S/N 029 forward polar boss midsect
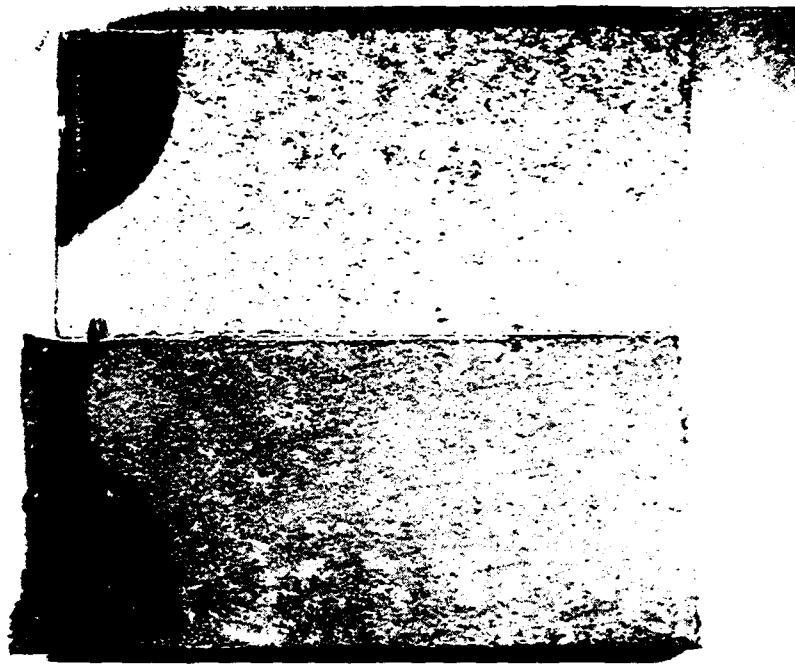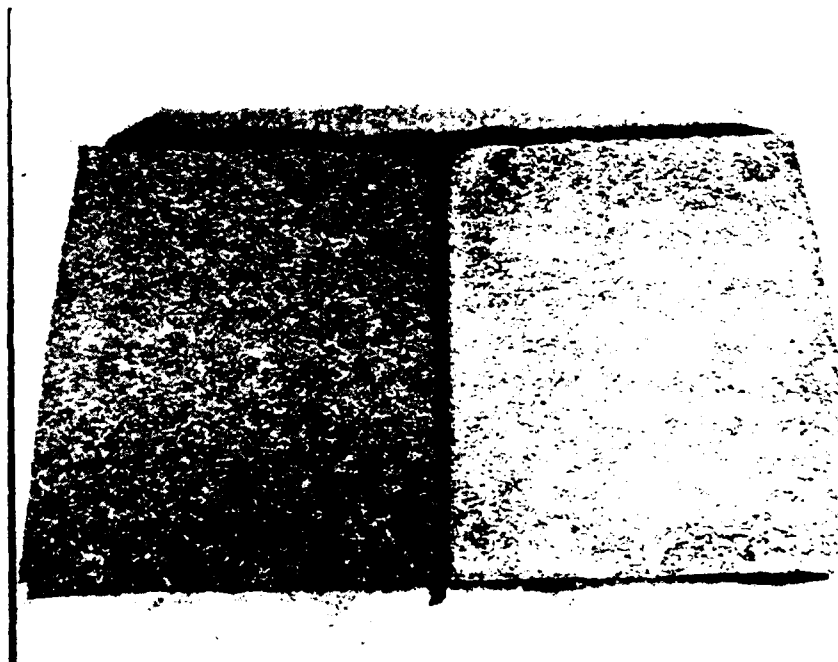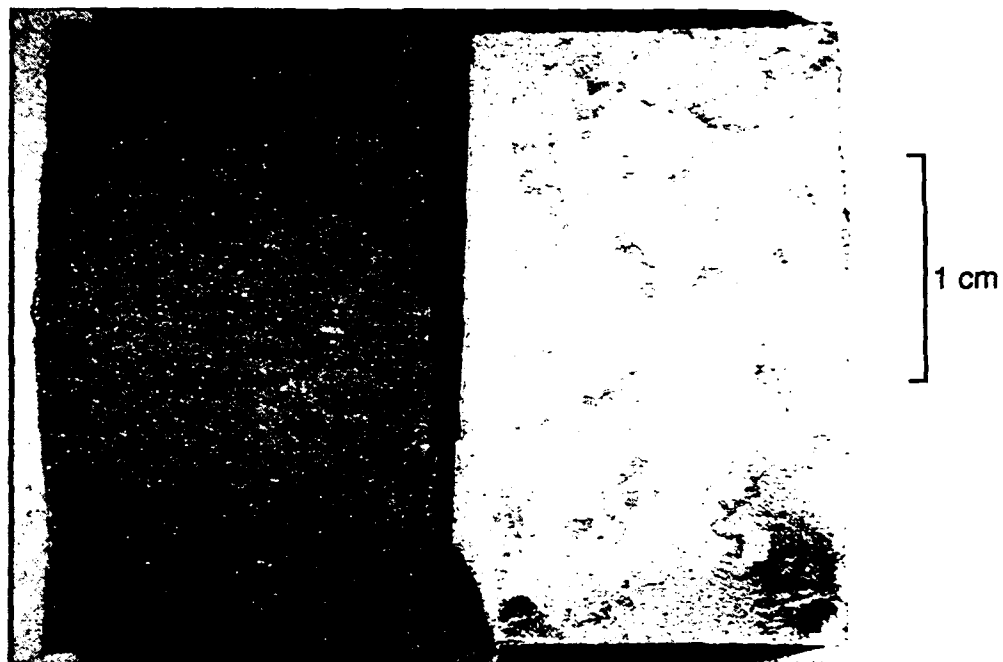Figure 4. Ruptured "good" bondline from S/N 029 forward polar boss midsection.

a

1 cm

b

1 cm

Figure 5. Ruptured "poor" bondlines. a) S/N 114 aft polar boss. b) S/N 029 aft polar boss.
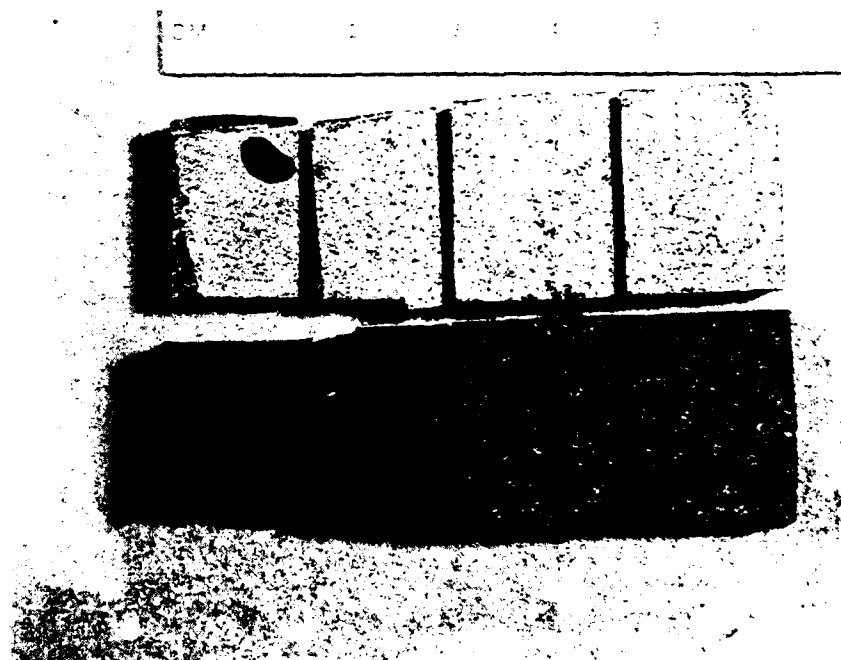
13

Figure 6. a) Ruptured "fair" bondline from S/N 126 aft polar boss. b) Ruptured bondline progresses from "fair" to "poor" from ID edge (left) to midsection, S/N 114 aft polar boss.

(segment A9). Figure 6b shows the progression from fair to poor in the condition of the bondline of the S/N 114 aft polar boss (segment A12), moving from the ID edge (left side) to the midsection. The progression is most readily seen in the exposed EPDM rubber surfaces of the coupons.

The appearance of the ruptured bondlines was distinctly different from the pulled-rubber bondlines, both for "good" and "poor" bonds. In the case of a pulled good bond, the rupture appeared to be cohesive within the EPDM. In the case of a pulled poor bond, rupture took place near the Al surface. The surface of both Al and insulation appeared spotted, as with a corrosion product, but a large area percentage of the Al side was covered with the Chemlok system after the insulation was pulled. Shallow surface lapping and polishing of such Al surface areas, which remained coated after peeling, showed a high density of corrosion product below the adhesive layer, and infiltrated into the primer layer.[6] Another observation, obscured on the pulled-rubber bondlines, was made on the rubber side of the temperature-stress ruptured bondlines. Many of the ruptured samples had faint patterns of parallel light brown streaks or grid patterns visible on the grey primer surface at the locus of failure. The patterns resembled brush strokes, and appeared to be bleed-through from the adhesive application (see Ref. 6, Table 3). Such a streaking pattern is seen clearly on the rubber side in Fig. 6a. Areas of corrosion product were often associated with the streaks, even on relatively good bondlines.

The XPS surface composition data for the IUS polar boss samples are shown in Table III. Information is provided in Table III about the method of rupture, the air exposure time before analysis, and the approximate analysis position referenced to the ID edge of the polar boss as "0%" (the wingtip of the polar boss is at "100%" in this scheme). The majority of the analyses were made on the Al side of the ruptured bondline, but analyses of the EPDM side of the rupture were included in some cases for comparison.

All of the data in Table III are consistent with the observation that temperature stress rupture occurs predominantly close to the aluminum-to-primer interface. From 1 to 13% Al was detected on each ruptured surface, including the EPDM surfaces. The zinc concentrations, typically 0.5 to 1.5 atom %, and high chlorine concentrations, 5 to 24 atom %, are indicative of the primer component. The aluminum and EPDM sides of the ruptured interface have similar composition, with a 20 to 40% decrease in the Al concentration on the EPDM surface being the most consistent difference. After this observation was made, further analysis of the EPDM rubber was limited to save time and to minimize sample outgassing contamination of the vacuum chamber used for XPS analysis.

It was observed that the ruptured aluminum-to-insulation bondlines did not appear to change significantly upon exposure to air, even after several weeks. For example, the three coupons analyzed from segment A6 of the forward polar boss of S/N 114 were exposed to air for 0 minutes, 3 minutes, and 40 hours before analysis without any significant differences in composition or surface chemical states being detected. The ID area of the bondline for the aft polar boss S/N 114, segment A1, was analyzed twice, first after liquid nitrogen rupture and dry box handling and then after several weeks exposure to air. No significant difference in the results was observed. This increased the confidence level for comparison of all the XPS data available.

Significant differences in surface composition were observed between noncorroded and corroded polar boss bondline surfaces. The variation in surface concentrations of Al, O, Cl, and C were all notable. The atomic concentration ratio, Cl:Al, is listed in Table III, along with a simplified description of the visual appearance of the bondline as predominantly "good," "fair," or "poor," with respect to observed extent of corrosion. It is seen that in general there is an excellent correlation between the calculated Cl:Al atomic % ratio, and the visual characterization of the extent of corrosion. The Cl:Al ratio, which represents the primer to aluminum compound ratio at the locus of failure, varied from 0.4 to 47. With only a few exceptions, surfaces with a fair to good, noncorroded

15

| Spec. No. | S/N | Polar Boss | Side | Analysis Position[1] | Rupture | Air Exp.[2] | Al | O | Si | Zn | Cl | S | C | N | Cl:Al | Bond Line[3] |
|---|---|---|---|---|---|---|---|---|---|---|---|---|---|---|---|---|
| A5 | 114 | Fwd | Al | ID | LN2[4] | 0 | 6.0 | 20 | 0.7 | 1.0 | 14 | 0.4 | 57 | 0.4 | 2.4 | Fair |
| A5 | 114 | Fwd | Al | mid(20%) | LN2 | 0 | 5.8 | 20 | 0.6 | 1.1 | 14 | 0.6 | 56 | 1.4 | 2.5 | Fair |
| A5 | 114 | Fwd | Al | mid(30%) | LN2 | 0 | 7.2 | 22 | 0.7 | 1.3 | 15 | 0.6 | 53 | 1.0 | 2.0 | Fair |
| A5 | 114 | Fwd | Al | mid(45%) | LN2 | 0 | 5.8 | 18 | 0.7 | 1.0 | 15 | 0.6 | 58 | 1.3 | 2.6 | Fair |
| A5 | 114 | Fwd | Al | mid(80%) | LN2 | 0 | 6.4 | 21 | 0.7 | 1.0 | 15 | 0.4 | 55 | 0.8 | 2.3 | Fair |
| A5 | 114 | Fwd | Al | wingtip | LN2 | 0 | 6.2 | 19 | 0.5 | 0.7 | 16 | 0.3 | 56 | 0.9 | 2.6 | Fair |
| A6 | 114 | Fwd | Al | ID | LN2 | 3 min | 4.6 | 20 | 0.8 | 1.0 | 13 | 0.2 | 61 | 0.5 | 2.8 | Fair |
| A6 | 114 | Fwd | EPDM | ID | LN2 | 3 min | 3.7 | 18 | 0.7 | 1.0 | 13 | 0.3 | 63 | 0.7 | 3.5 | Fair |
| A6 | 114 | Fwd | Al | mid(40%) | LHe[5] | 40 hr | 6.3 | 21 | 0.5 | 1.1 | 13 | 0.5 | 57 | 0.8 | 2.1 | Fair |
| A6 | 114 | Fwd | EPDM | mid(40%) | LHe | 40 hr | 5.0 | 20 | 0.4 | 1.2 | 13 | 0.4 | 60 | 0.9 | 2.6 | Fair |
| A6 | 114 | Fwd | Al | mid(60%) | LN2 | 0 | 6.8 | 23 | 0.6 | 1.3 | 14 | 0.4 | 54 | 0.7 | 2.1 | Fair |
| A6 | 114 | Fwd | EPDM | mid(60%) | LN2 | 0 | 4.0 | 16 | 0.5 | 0.7 | 9.1 | 0.6 | 68 | 1.2 | 2.3 | Fair |
| A1 | 114 | Aft | Al | ID | LN2 | 0 | 6.7 | 25 | 0.6 | 1.0 | 6.1 | 0.7 | 59 | 1.4 | 0.9 | Fair |
| A1 | 114 | Aft | Al | ID | LN2 | >1 wk | 7.0 | 26 | 0.5 | 1.3 | 7.7 | 0.5 | 56 | 1.0 | 1.1 | Poor |
| A1 | 114 | Aft | Al | mid(20%) | LN2 | >1 wk | 6.3 | 26 | 0.4 | 1.3 | 5.5 | 0.8 | 59 | 1.3 | 0.9 | Poor |
| A1 | 114 | Aft | Al | mid(40%) | LN2 | 20 hr | 9.1 | 29 | 0.1 | 1.1 | 5.8 | 1.0 | 52 | 1.3 | 0.6 | Poor |
| A1 | 114 | Aft | EPDM | mid(40%) | LN2 | 23 hr | 6.8 | 24 | 1.0 | 0.9 | 5.5 | 1.2 | 59 | 2.1 | 0.8 | Poor |
| A1 | 114 | Aft | Al | mid(80%) | LN2 | >1 wk | 9.8 | 28 | 0.6 | 1.2 | 5.0 | 1.4 | 52 | 1.7 | 0.5 | Poor |
| A1 | 114 | Aft | Al | wingtip | LN2 | >1 wk | 7.8 | 25 | 0.4 | 1.1 | 7.7 | 1.0 | 55 | 2.0 | 1.0 | Fair |
| A2 | 114 | Aft | Al | ID | LN2 | 0 | 9.3 | 26 | 0.7 | 1.4 | 9.6 | 0.5 | 52 | 0.5 | 1.0 | Poor |
| A2 | 114 | Aft | Al | mid(20%) | LN2 | 0 | 7.8 | 22 | 0.5 | 1.2 | 13 | 0.7 | 53 | 1.1 | 1.7 | Fair |
| A2 | 114 | Aft | Al | mid(30%) | LN2 | 0 | 7.6 | 24 | 0.6 | 1.4 | 11 | 0.9 | 53 | 1.3 | 1.5 | Fair |
| A2 | 114 | Aft | Al | mid(80%) | LN2 | 0 | 12 | 31 | 0.8 | 1.2 | 5.6 | 1.1 | 47 | 1.4 | 0.5 | Poor |
| A2 | 114 | Aft | Al | mid(90%) | LN2 | 0 | 11 | 29 | tr | 0.8 | 7.5 | 0.9 | 49 | 1.3 | 0.7 | Poor |
| A12 | 114 | Aft | Al | ID | LN2 | 0 | 4.8 | 19 | 0.7 | 0.9 | 12 | 0.7 | 61 | 1.2 | 2.6 | Fair |
| A12 | 114 | Aft | Al | mid(25%) | LN2 | 0 | 7.0 | 27 | 0.3 | 1.3 | 9.4 | 0.7 | 54 | 1.2 | 1.3 | Fair |
| A12 | 114 | Aft | Al | mid(40%) | LN2 | 0 | 9.4 | 30 | 0.6 | 1.2 | 5.7 | 1.0 | 50 | 1.4 | 0.6 | Poor |
| A12 | 114 | Aft | Al | mid(60%) | LN2 | 0 | 11 | 33 | 0.2 | 1.2 | 3.8 | 1.2 | 48 | 1.2 | 0.4 | Poor |
| A7 | 029 | Fwd | Al | mid(10%) | LN2 | 5 min | 2.2 | 13 | 2.1 | 0.3 | 15 | 0.3 | 66 | 0.6 | 6.8 | Good |
| A7 | 029 | Fwd | Al | mid(60%) | LN2 | >1 wk | 1.9 | 11 | 0.3 | 0.6 | 19 | 0.4 | 66 | 0.9 | 10 | Good |
| A8 | 029 | Fwd | Al | ID | LN2 | 0 | 2.0 | 12 | 3.4 | 0.7 | 19 | 0.4 | 62 | tr | 9.6 | Good |
| A8 | 029 | Fwd | Al | mid(20%) | LN2 | 0 | 2.3 | 11 | 0.9 | 0.8 | 20 | 0.4 | 64 | 0.6 | 8.6 | Good |
| A8 | 029 | Fwd | Al | mid(30%) | LN2 | 0 | 3.3 | 11 | 0.7 | 0.9 | 11 | 0.4 | 72 | 0.5 | 3.4 | Good |
| A8 | 029 | Fwd | Al | mid(45%) | LN2 | 0 | 3.1 | 11 | 0.6 | 1.0 | 20 | 0.6 | 63 | 0.9 | 6.5 | Good |
| A8 | 029 | Fwd | Al | mid(80%) | LN2 | 0 | 3.9 | 12 | 0.5 | 0.6 | 19 | 0.4 | 62 | 0.4 | 5.0 | Good |
| A8 | 029 | Fwd | Al | wingtip | LN2 | 0 | 2.0 | 8.6 | 0.6 | 0.8 | 18 | 0.5 | 69 | 0.5 | 8.9 | Good |

16

| Spec. No. | | | Sample Description | | | Surface Atomic Percent, Normalized | | | | | | | | Bond Line |
|---|---|---|---|---|---|---|---|---|---|---|---|---|---|---|
| | S/N | Polar Boss | Side | Analysis Position | Rupture | Air Exp. | Al | O | Si | Zn | Cl | S | C | N | Cl:Al | |
| A3 | 029 | Aft | Al | mid(15%) | LN2 | 0 | 5.1 | 15 | 1.0 | 0.6 | 8.9 | 0.9 | 67 | 1.3 | 1.8 | Fair |
| A3 | 029 | Aft | Al | mid(20%) | LN2 | 0 | 9.0 | 22 | 0.5 | 0.6 | 6.8 | 0.8 | 59 | 1.2 | 0.8 | Poor |
| A3 | 029 | Aft | Al | mid(30%) | LN2 | 0 | 8.5 | 21 | 0.7 | 0.5 | 5.2 | 0.6 | 62 | 1.2 | 0.6 | Poor |
| A3 | 029 | Aft | Al | mid(45%) | LN2 | 0 | 8.4 | 21 | 0.7 | 0.6 | 6.8 | 0.7 | 60 | 1.2 | 0.8 | Poor |
| A3 | 029 | Aft | Al | mid(80%) | LN2 | 0 | 13 | 29 | 0.5 | 0.7 | 7.4 | 0.7 | 48 | 1.6 | 0.6 | Poor |
| A3 | 029 | Aft | Al | mid(90%) | LN2 | 0 | 11 | 27 | 0.2 | 0.6 | 8.7 | 0.8 | 50 | 1.6 | 0.8 | Poor |
| A4 | 029 | Aft | Al | ID | LN2 | 0 | 3.3 | 18 | 3.2 | 0.6 | 11 | 0.3 | 63 | 0.9 | 3.4 | Fair |
| A4 | 029 | Aft | Al | mid(20%) | LN2 | 0 | 6.9 | 24 | 1.1 | 0.6 | 8.2 | 0.3 | 58 | 0.9 | 1.2 | Fair |
| A4 | 029 | Aft | Al | mid(40%) | LN2 | 20 hr | 9.3 | 28 | 0.3 | 0.6 | 8.5 | 0.6 | 52 | 1.4 | 0.9 | Poor |
| A4 | 029 | Aft | Al | mid(80%) | LN2 | >1 wk | 8.5 | 27 | 0.3 | 0.7 | 7.3 | 0.7 | 54 | 1.5 | 0.9 | Poor |
| A4 | 029 | Aft | Al | wingtip | LN2 | >1 wk | 3.4 | 16 | 0.4 | 0.8 | 16 | 0.5 | 63 | 0.9 | 4.6 | Fair |
| A9 | 126 | Aft | Al | ID | LN2 | 0 | 0.5 | 5.8 | 0.3 | 0.2 | 24 | 0.4 | 68 | 0.9 | 47 | Good |
| A9 | 126 | Aft | Al | mid(20%) | LN2 | 0 | 3.4 | 11 | 0.3 | 0.6 | 19 | 0.7 | 63 | 1.4 | 5.6 | Fair |
| A9 | 126 | Aft | Al | mid(30%) | LN2 | 0 | 3.9 | 12 | 0.4 | 0.6 | 20 | 1.0 | 61 | 1.0 | 5.2 | Fair |
| A9 | 126 | Aft | Al | mid(45%) | LN2 | 0 | 4.2 | 13 | n.d. | 0.6 | 21 | 1.0 | 60 | 0.8 | 4.9 | Fair |
| A9 | 126 | Aft | Al | mid(55%) | LN2 | 0 | 5.4 | 18 | 0.5 | 0.6 | 14 | 1.6 | 58 | 1.9 | 2.5 | Fair |
| A9 | 126 | Aft | Al | mid(70%) | LN2 | 0 | 3.3 | 14 | 0.7 | 0.7 | 18 | 0.9 | 61 | 1.4 | 5.3 | Fair |

Notes: 1. Analysis Position is defined as an approximate percentage of the distance from the ID edge (5%) to the wingtip (95%) along a polar boss radius.

2. Air Exp. = Air exposure time between rupture and introduction to vacuum; a "0" time indicates that the sample was handled in an inert atmosphere dry box.

3. Bond Line =Appearance of bond line after rupture.
   a. Good = Metal and rubber surfaces look clean; infrequent small patches of corrosion.
   b. Fair = Rubber surface looks clean, but metal surface is lightly mottled; small patches of corrosion product.
   c. Poor = Metal and rubber surfaces look mottled; high density of patches of corrosion product, some large.

4. LN2 = Liquid nitrogen.

5. LHe = Liquid helium.

appearance had Cl:Al ratios > 2, and surfaces with a poor, corroded appearance had Cl:Al ratios < 1. The change in this ratio was related to changes in both the Al and Cl concentrations. As the bondline changed from good to bad, the Al oxide/hydroxide concentration increased significantly and the primer concentration, represented by the covalently bonded Cl signal, decreased.

All samples from the forward polar bosses of both S/N 114 and 029, and from the aft polar boss of S/N 126, had a relatively noncorroded appearance on the ruptured surfaces. For example, except for about 2% Al, the composition on the forward polar boss S/N 029 surfaces is comparable to the Chemlok 205 primer composition seen in Table II. The surface chlorine was predominantly bonded to carbon; low levels of chloride would not be distinguished. The aluminum was detected only as oxide and/or hydroxide, but low levels of aluminum chloride would not be distinguished in a mixture.

In comparison, the S/N 114 forward polar boss ruptured surfaces had higher concentrations of Al and O, and lower concentrations of Cl and C. Significant differences for all these elements are now observed with comparison to the primer composition. The Cl:Al ratio for the Al side of the rupture ranged from 2 to 3. The simplest interpretation of the data is that there are higher concentrations of aluminum oxide/hydroxide at the rupture zone. If the rupture is occurring close to the aluminum-to-primer interface, an increase in aluminum oxide/hydroxide formation there is being observed. It is reasonable to expect that areas of thickened, brittle aluminum oxide/hydroxide would be more susceptible to temperature-stress rupture than the primer layer or a non-corroded aluminum-to-primer bond. This would be particularly true if the corrosion product is infiltrated into a network of cracks in the primer layer,[4,6] which would provide a weakened zone for rupture propagation. The visual appearance of the S/N 114 forward polar boss samples and the S/N 126 aft polar boss samples (midsection) was comparable. The XPS data suggested that the S/N 126 aft polar boss bondline was less corroded than the forward polar boss bondline of S/N 114 in that it had less aluminum oxide/hydroxide.

The aft polar boss segments analyzed from both S/N 114 and 029 were characterized by the appearance of corrosion over the entire mid-section of the ruptured aluminum to insulation bondline. The ID edges and wingtip edges of the aft segments appeared less corroded than the mid-sections in each case except the A2 segment from S/N 114. The XPS data in Table III shows a trend of decreasing Cl:Al atomic % ratio from the edges of the segments to the mid-section. There were significant differences from segment to segment. The ID edge of the aft segment from S/N 126 had a Cl:Al atomic ratio of 47. The edges of the A4 segment from the S/N 029 aft polar boss had Cl:Al ratios of 3.4 and 4.6. Finally, the edges of the A1 and A2 segments from the S/N 114 aft polar boss had low Cl:Al ratios of 1.0. If the bondline description was based on the XPS analysis results, these edges would be ranked as significantly corroded. The Table III data suggested that XPS is a more sensitive probe of the extent of corrosion at the bondline than just a visual inspection of the ruptured surfaces. As on the forward polar boss samples, no chloride was distinguished from the XPS chlorine signal, but its presence at low concentration is not ruled out.

The aft segment corroded bondline sections appeared to have significantly higher concentrations of aluminum oxide/hydroxide than the relatively noncorroded areas. The temperature-stress rupture appeared to progress most readily through areas of thickened aluminum oxide/hydroxide if it was present. These areas of corrosion product were also noted to be correlated with pockets of primer pull-out from the rubber side of the rupture.[4] This would be consistent with the infiltration of corrosion product into a network of cracks in the primer layer.[6] It is possible that such crack defects in the primer layer determine the initiation sites for the metal corrosion. The pattern of corrosion on the aft polar bosses (ID and wingtip edges less corroded than the midsections), and the significant

18

differences observed between the forward and aft bosses exposed to comparable storage environments, strongly suggest a manufacturing-process-related initiation of corrosion. This, in turn, implies that properly stored flight motors, regardless of age, need to be inspected for the presence of corrosion.

XPS data is available on a few polar boss samples where the bondline was ruptured by peeling the insulation from the aluminum.[7] Although the surface analysis was complicated by large areas of cohesive failure, the Cl:Al ratio for the three samples analyzed from the mid-section of the S/N 114 aft polar boss were 0.1, 0.3, and 1.3. This is in good agreement with the data in Table III. The peeled sample from the S/N 114 forward polar boss apparently failed predominantly in the rubber: the results from Surface Science Laboratories showed no aluminum detected and low chlorine concentration.

A few additional comments can be made about the XPS results. On average, the N and S concentrations tended to be somewhat higher on the corroded surfaces than on the noncorroded surfaces, but the differences were fairly small and inconsistencies were observed. Some "sulfate" (highly oxidized) sulfur was observed on most of the samples analyzed, typically about 25% of the total sulfur. The concentration of zinc oxide was higher on most of the ruptured surfaces than on the reference primer samples. This might be due to the details of how temperature-shock rupture occurs through the primer (e.g., rupture might occur preferentially near the zinc oxide particles), or there may be some segregation of zinc oxide at the interface. The titanium oxide was not detected by XPS on any of the ruptured surfaces. The C1s spectra of the ruptured surfaces with high Cl:Al atomic % ratio appeared comparable to the C1s spectrum of the reference primer material, (i.e.,a large shoulder at higher binding energy due to chlorine and oxygen bonded to the carbon). The C1s spectra of the ruptured surfaces with lower Cl:Al atomic % ratio had much smaller shoulders at higher binding energy, implying that a significant fraction of the surface carbon for these samples is not associated with primer material. This carbon may in part be starting contamination on the aluminum surface before it is coated with primer.

## CONCLUSIONS

A temperature-stress rupture method using partial immersion in liquid nitrogen has been developed for the aluminum/EPDM rubber insulation bondline of the IUS SRM-1 polar bosses. XPS analysis of reference materials showed that the technique could successfully distinguish all layers of the bondline, including the Chemlok primer and adhesive. Subsequent XPS analysis of the ruptured bondlines followed changes at the locus of failure as corrosion progressed.

The variation in surface concentrations of Al, O, Cl, and C were notable when corroded and noncorroded bondlines were compared. In general there was a very good correlation between the calculated Cl:Al atomic % ratio, and the visual characterization of the extent of corrosion. The Cl:Al ratio, which represents the primer to corrosion product ratio at the locus of failure, varied from 0.4 to 47. With only a few exceptions, surfaces with a predominantly noncorroded appearance had Cl:Al ratios > 2, and surfaces with a heavily corroded appearance had Cl:Al ratios < 1. The change in this ratio is related to changes in both the Al and Cl concentrations. As the bondline changed from good to poor, the Al increased significantly and the Cl decreased. The corroded bondline sections appeared to have significantly higher concentrations of aluminum oxide/hydroxide than the noncorroded areas, and lower concentrations of primer material. The temperature-stress rupture appeared to progress most readily through areas of thickened aluminum oxide/hydroxide when it was present. The corrosion product was infiltrated into a network of cracks in the primer layer, which provided a weakened zone for rupture propagation.

All samples from the forward polar bosses of both S/N 114 and 029, and from the aft polar boss of S/N 126, had a relatively noncorroded appearance on the ruptured surfaces. The aft polar boss segments analyzed from both S/N 114 and 029 were characterized by the appearance of corrosion over the entire mid-section of the ruptured aluminum to insulation bondline. The ID edges and wingtip edges of the aft segments appeared to be less corroded than the mid-sections, but the XPS data suggests that the surface composition analysis technique is a more sensitive probe of the extent of corrosion at the bondline than a visual inspection of the ruptured surfaces. The XPS data showed a clear trend of relatively high Cl:Al ratio for the forward polar boss samples and decreasing Cl:Al atomic % ratio from the edges of the aft polar boss segments to the mid-sections. The pattern of corrosion on the aft polar bosses, and the significant differences observed between the forward and aft bosses exposed to comparable storage environments, strongly suggest a manufacturing-process-related initiation of corrosion. This, in turn, implies that properly stored flight motors, regardless of age, need to be inspected for the presence of corrosion. Corrosion may initiate at cracks in the primer layer. Streaking patterns observed in the primer layer may be indicative of nonuniform application of the primer or adhesive layers.

No chloride was distinguished from the XPS chlorine signal on any of the polar boss samples, but its presence at low concentration was not ruled out. Some "sulfate" (highly oxidized) sulfur was observed on most of the samples analyzed, typically about 25% of the total sulfur. The concentration of zinc oxide was higher on most of the ruptured surfaces than on the reference primer samples. This might be due to the details of how temperature-shock rupture occurs through the primer (e.g., rupture might occur preferentially near the zinc oxide particles), or there may be some segregation of zinc oxide at the interface.

## REFERENCES

1. S. Zacharius, W. Stuckey, G. Cagle and C. Hemminger, "Interfacial Chemistry in Metal-to-Rubber Bonds." Presented at the Thirteenth Annual Meeting of the Adhesion Society, February 1990.

2. C. S. Hemminger, "XPS Analysis of Temperature-Shock Ruptured Al/EPDM Bondlines from IUS SRM-1 Polar Bosses," ATM No. 92(2464-05)-3 (25 February 1992).

3. C. S. Hemminger, "Effect of Water on EPDM Rubber/Aluminum Bonded with Chemlok Adhesive System: Modified Test Plan," IOC No. 92-5654-CSH-6 (6 February 1992).

4. C. S. Hemminger and N. Marquez, "Effect of Water on EPDM Rubber/Aluminum Bonded with Chemlok Adhesive System: Final Report," Aerospace Report No. TOR-92(2464)-4 (30 September 1992).

5. Chemical Systems Division of United Technologies, Specification No. SE0865B, "Insulation, Rubber, Bonding and Fabrication of, IUS Program," (16 June 1982).

6. S. W. Frost, T. D. Le, and R. A. Brose, "Metallurgical Evaluation of Bondline Corrosion on Aluminum Polar Bosses from IUS Insulated Motor Cases," The Aerospace Corporation ATM No. 92(2464-05)-5 (10 March 1992).

7. C. S. Hemminger, "XPS Interface Analysis: EPDM Rubber/Aluminum Bonded with Chemlok Adhesive System," IOC No. 92-5654-CSH-04 (8 January 1992).

# TECHNOLOGY OPERATIONS

The Aerospace Corporation functions as an "architect-engineer" for national security programs, specializing in advanced military space systems. The Corporation's Technology Operations supports the effective and timely development and operation of national security systems through scientific research and the application of advanced technology. Vital to the success of the Corporation is the technical staff's wide-ranging expertise and its ability to stay abreast of new technological developments and program support issues associated with rapidly evolving space systems. Contributing capabilities are provided by these individual Technology Centers:

**Electronics Technology Center:** Microelectronics, solid-state device physics, VLSI reliability, compound semiconductors, radiation hardening, data storage technologies, infrared detector devices and testing; electro-optics, quantum electronics, solid-state lasers, optical propagation and communications; cw and pulsed chemical laser development, optical resonators, beam control, atmospheric propagation, and laser effects and countermeasures; atomic frequency standards, applied laser spectroscopy, laser chemistry, laser optoelectronics, phase conjugation and coherent imaging, solar cell physics, battery electrochemistry, battery testing and evaluation.

**Mechanics and Materials Technology Center:** Evaluation and characterization of new materials: metals, alloys, ceramics, polymers and their composites, and new forms of carbon; development and analysis of thin films and deposition techniques; nondestructive evaluation, component failure analysis and reliability; fracture mechanics and stress corrosion; development and evaluation of hardened components; analysis and evaluation of materials at cryogenic and elevated temperatures; launch vehicle and reentry fluid mechanics, heat transfer and flight dynamics; chemical and electric propulsion; spacecraft structural mechanics, spacecraft survivability and vulnerability assessment; contamination, thermal and structural control; high temperature thermomechanics, gas kinetics and radiation; lubrication and surface phenomena.

**Space and Environment Technology Center:** Magnetospheric, auroral and cosmic ray physics, wave-particle interactions, magnetospheric plasma waves; atmospheric and ionospheric physics, density and composition of the upper atmosphere, remote sensing using atmospheric radiation; solar physics, infrared astronomy, infrared signature analysis; effects of solar activity, magnetic storms and nuclear explosions on the earth's atmosphere, ionosphere and magnetosphere; effects of electromagnetic and particulate radiations on space systems; space instrumentation; propellant chemistry, chemical dynamics, environmental chemistry, trace detection; atmospheric chemical reactions, atmospheric optics, light scattering, state-specific chemical reactions and radiative signatures of missile plumes, and sensor out-of-field-of-view rejection.